Available online at www.sciencedirect.com
ScienceDirect
Bioorganic & Medicinal Chemistry 16 (2008) 5322–5330
Bioorganic & Medicinal Chemistry

Chemical and biological investigation of *N*-hydroxy-valdecoxib: An active metabolite of valdecoxib

Péter Erdélyi,[a,*] Tamás Fodor,[a] Ágnes Kis Varga,[b] Mátyás Czugler,[c] Anikó Gere[b] and János Fischer[a]

[a]*Medicinal Chemistry Research Laboratory No. IV., Gedeon Richter Plc., PO Box 27, H-1475 Budapest 10, Hungary*
[b]*Department of Pharmacology, Gedeon Richter Plc., PO Box 27, H-1475 Budapest 10, Hungary*
[c]*X-ray Diffraction Department, Institute of Structural Chemistry, Chemical Research Center, Hungarian Academy of Sciences, Pusztaszeri út 59-67, 1025 Budapest, Hungary*

Received 14 October 2007; revised 25 February 2008; accepted 28 February 2008
Available online 4 March 2008

Abstract—The inhibition of cyclooxygenase enzymes plays an important role in the treatment of inflammatory diseases. *N*-Hydroxy-4-(5-methyl-3-phenylisoxazol-4-yl)benzenesulfonamide (**3**)—a primary metabolite of the highly selective COX-2 inhibitor valdecoxib—was synthesized and stabilized as its monohydrate (**3a**·H_2O). The anti-inflammatory properties of **3a**·H_2O were investigated in carrageenan-induced edema and in acute and chronic pain models. Based on our biological investigation, we conclude that *N*-hydroxy-valdecoxib **3a** is an active metabolite of valdecoxib.

1. Introduction

Non-steroidal anti-inflammatory drugs (NSAIDs) are widely used in the treatment of diseases accompanied by rheumatic inflammation, pain, and fever. The action of these compounds are based on the inhibition of the enzyme cyclooxygenase (COX), sometimes referred to as prostaglandin synthase.[1] Prostaglandins (PGs) are lipid compounds derived from fatty acids that are produced by most cells in the body and are present in virtually all human organs and tissues. PGs are considered to be mediators with a variety of strong physiological effects such as platelet aggregation and gastrocytoprotection. Another important function of PGs is the response of the human tissue to inflammation and injury. They play a significant role in symptoms accompanied by inflammation: swelling, redness, and pain because of the increased vascular permeability and the sensitized peripheral nerve endings and additionally fever is also mediated by PGs. It was determined that the levels of PGs are appreciably elevated in inflamed tissues compared to normal tissues.[2] The synthesis of PGs is determined by COX enzymes, the amount of which is mediated by the cytokines selected by the stimulated cells. The cyclooxygenase enzyme exists in two isoforms: cyclooxygenase-1 (COX-1) and cyclooxygenase-2 (COX-2).[3,4] Further experiments including the cloning of COX-2 led to the realization that COX-1 is constitutively expressed in essentially all tissues whereas COX-2 is induced by inflammatory stimuli.[5–7] It is known that the latter is responsible for the conversion of arachidonic acid to prostaglandin H_2, the key mediator of inflammation.[8] The long term use of NSAIDs is limited by gastrointestinal side effects such as dyspepsia and abdominal pain, and less often, gastric or duodenal perforation and bleeding.[9] Coxibs, the highly COX-2 selective second generation of NSAIDs, were developed to achieve a better gastrointestinal adverse effect profile; however, these side effects could only be reduced. The first member of coxibs is celecoxib an *ortho*-diaryl-heterocyclic structure was launched in 1999[10] (Scheme 1). In the recent years, however most of the coxibs have been withdrawn from the market because of their unexpected cardiovascular effects.

The scope of our research programme was to find novel selective COX-2 inhibitors with a better side effect profile by the method of analogue based drug discovery[11] using valdecoxib[12] (Scheme 1) as a lead compound.

Keywords: Valdecoxib analogues; Cyclooxygenase-2 inhibitor; COX-2; Active metabolite; Non-steroidal anti-inflammatory drugs.
* Corresponding author. Tel.: +36 1 889 8711; e-mail: p.erdelyi@richter.hu

0968-0896/$ - see front matter © 2008 Elsevier Ltd. All rights reserved.
doi:10.1016/j.bmc.2008.02.088

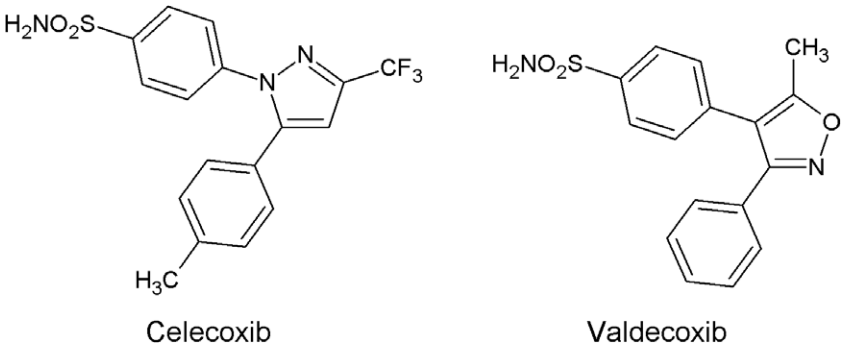

Scheme 1. Celecoxib and valdecoxib.

The close analogues of celecoxib and rofecoxib have already been reported in this journal by others.[13,14]

2. Chemistry

Several novel direct analogues of valdecoxib were prepared and their pharmacological properties were studied in vitro and in vivo. *N*-Hydroxy-4-(5-methyl-3-phenylisoxazol-4-yl)benzenesulfonamide (*N*-hydroxy-valdecoxib) (**3**) was found to be the only effective compound among these analogues. It has been reported earlier that valdecoxib transforms in primary oxidative metabolic pathways to *N*-hydroxy-valdecoxib through *N*-hydroxylation at the sulfonamide moiety in mice[15] and in humans.[16]

There are no synthetic and biological data on this metabolite of valdecoxib. The present work reports on its synthesis and biological investigations.

Compound **3** was prepared according to the procedure outlined in Scheme 2. 5-Methyl-3,4-diphenylisoxazole (**1**)[12] was chlorosulfonated to give a mixture of isomers **2a** and **2b**. Recrystallization from cyclohexane afforded the pure 4-isomer, which was treated with hydroxylamine hydrochloride in dioxane to give **3** in a good yield.

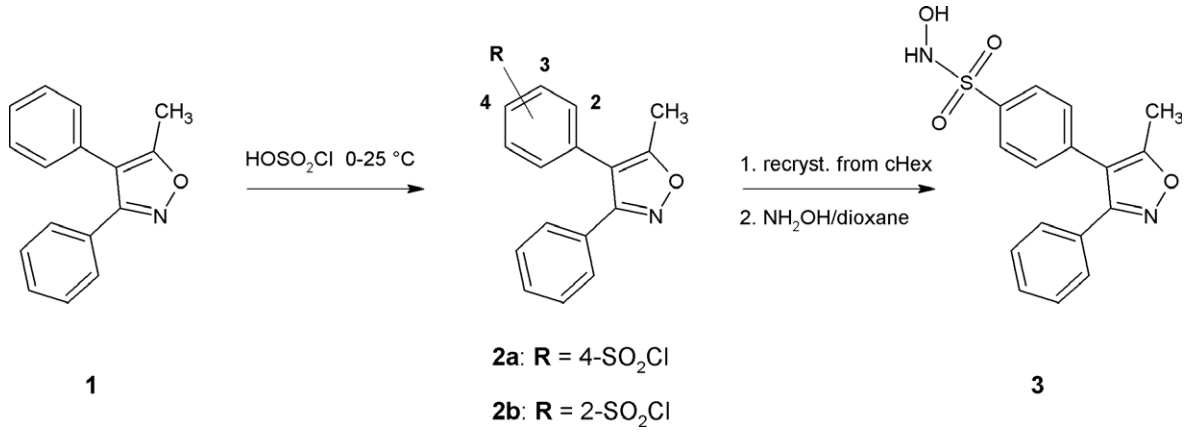

Scheme 2. The synthesis of *N*-hydroxy-valdecoxib (**3**).

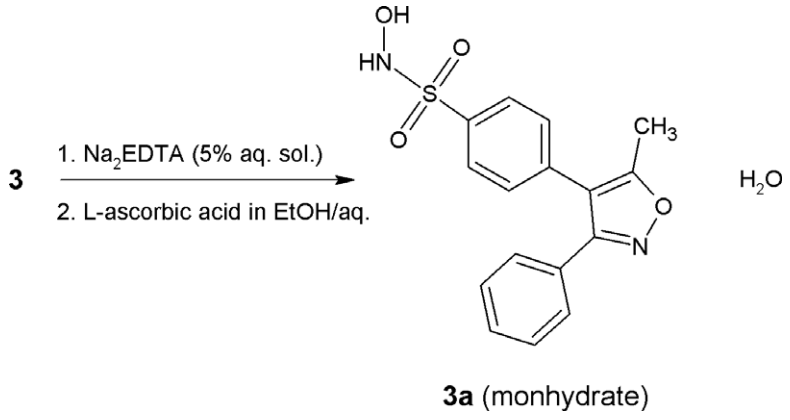

Scheme 3. The preparation of *N*-hydroxy-valdecoxib monohydrate (**3a**·H_2O).

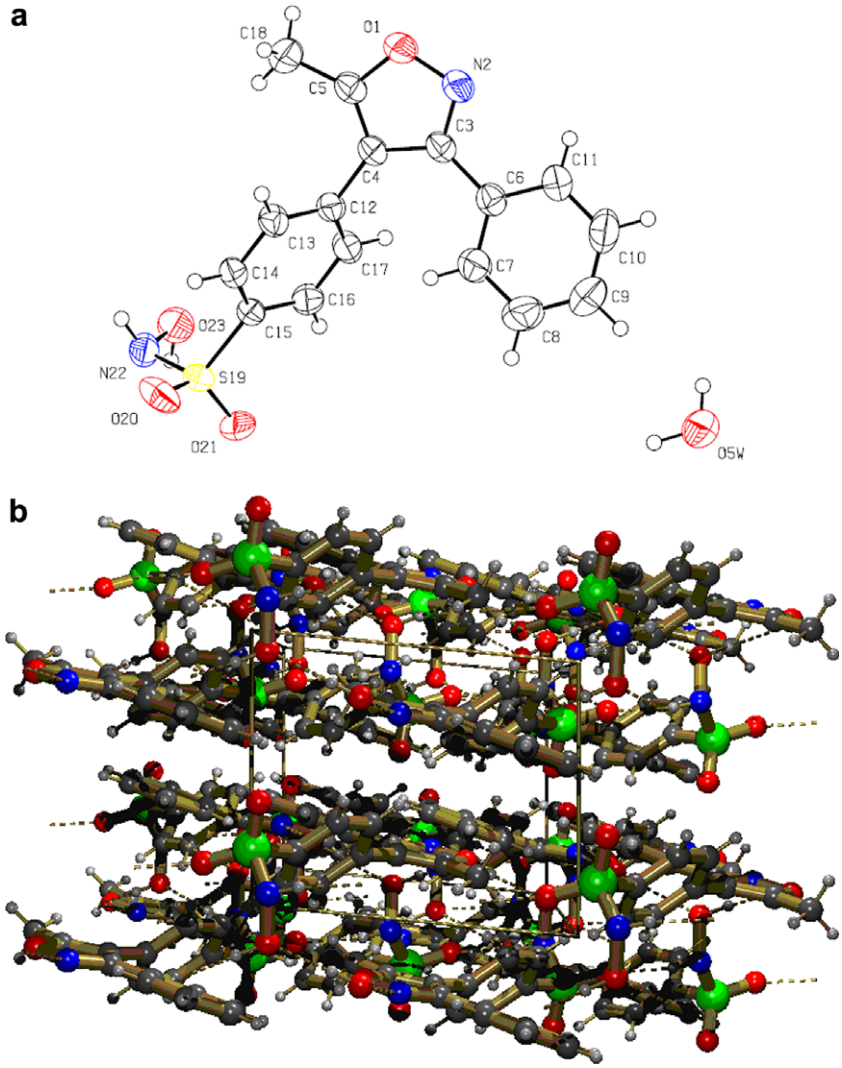

Figure 1. (a) Molecular structure of **3a**·H_2O with 50% probability anisotropic displacement ellipsoids. (b) Packing in the crystal structure of **3a**·H_2O as seen along the *b* crystallographic axis. Hydrophilic layers formed at near to $x \sim 0$ are visible while apolar (hydrophobic) surfaces are clearly exposed at around $x \sim 1/2$.

Unfortunately, stability problems were observed with *N*-hydroxy-valdecoxib (**3**) prepared as described above via a fast decomposition to the sulfinic acid derivative at room temperature. Other aromatic *N*-hydroxysulfonamides such as Piloty's acid (*N*-hydroxy-benzenesulfonamide) decompose while nitroxyl (HNO) is generated.[17] If crude *N*-hydroxy-valdecoxib (**3**) was dissolved in EtOAc and treated with Na_2EDTA solution to remove chelating metal ion traces, and crystallized from a dilute solution of L-ascorbic acid in aqueous ethanol, **3** was isolated as a stable monohydrate (**3a**·H_2O) whose water content remained constant at room temperatures (under standard humidity conditions) over a period of two years (Scheme 3). According to TGA and DSC analysis **3a**·H_2O decomposed to afford one mole of water between 93 and 160 °C and a fast decomposition occurred at 180 °C. We have also found other stable solvates of **3**, whose preparation and structure determinations by X-ray crystallography will be reported elsewhere. The molecular structure of **3a**·H_2O as seen from the crystal structure is shown in Figure 1a. The crystal structure is characterized by a double-layer like arrangement of the hydrogen-bonded array of the associated **3** molecules and water (cf. Fig. 1a and b) yielding to such layers. These double-layer like formations with their polar core and apolar exterior are then combined into making the macroscopic crystal.

3. Pharmacology

The effect of *N*-hydroxy-valdecoxib monohydrate (**3a**·H_2O) on human COX-2 inhibition was 28 times

Table 1. In vitro efficacity of valdecoxib and **3a**·H_2O in the TMPD assay

Compound	$IC_{50} \pm$ SEM (μM)		
	Human recombinant COX-2	Ovine COX-1	COX-1/ COX-2 selectivity
Valdecoxib	0.04 ± 0.02	157.2 ± 6.2	3930
3a	1.1 ± 0.2	96.2 ± 10.2	88

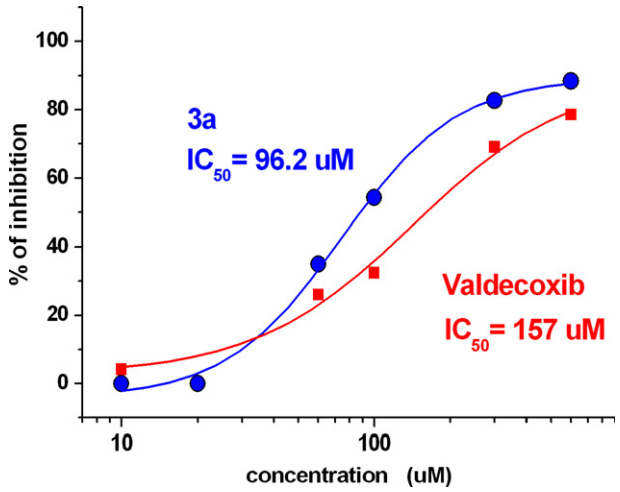

Figure 2. Inhibition effect on ovine COX-1 enzyme.

lower than that of valdecoxib, therefore, the COX-1/COX-2 selectivity of **3a**·H_2O was much lower than that of valdecoxib (Table 1 and Figs. 2 and 3). Compound **3a**·H_2O inhibited the LPS-induced PGE2 elevation significantly weaker than valdecoxib (Fig. 4).

Compound **3a**·H_2O had a dose dependent significant edema inhibition effect in the carrageenan-induced paw edema assay. It had an anti-edema effect at a dose of 0.3 mg/kg po whereas valdecoxib showed no inhibition at the same dose (Figs. 5 and 6).

The analgetic and anti-inflammatory activity was determined in rats in acute and chronic experiments. The carrageenan provoked mechanical hyperalgesia assay indicated that both compounds—valdecoxib and **3a**·H_2O—had considerable analgesic activity (Fig. 7). Compound **3a**·H_2O showed a significant analgesic activity for 3 h after treatment and it has a longer duration of action as compared with valdecoxib.

In the subchronic pain model, valdecoxib reached the efficacy of **3a**·H_2O only at a higher dose level (10 mg/kg vs 3 mg/kg), (Fig. 8). Valdecoxib and **3a**·H_2O have

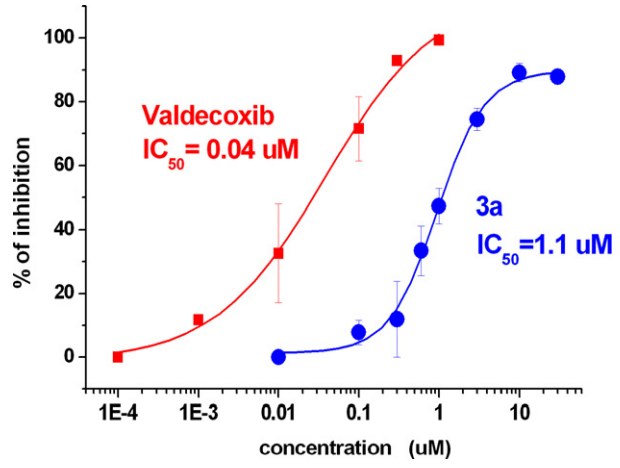

Figure 3. Inhibition effect on human COX-2 enzyme.

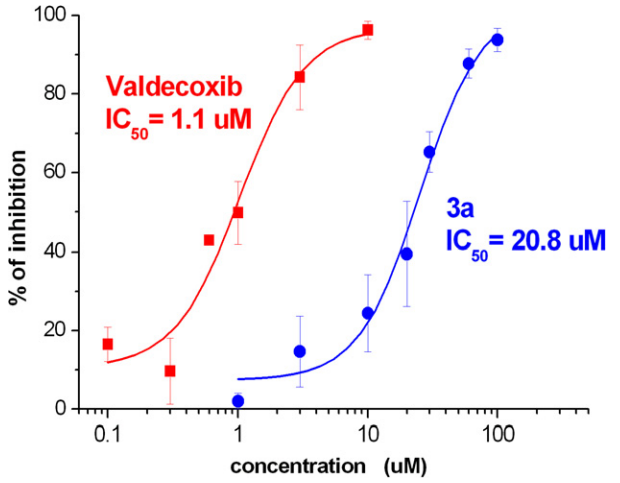

Figure 4. Effect of the test compounds in the LPS evoked PGE2 production assay.

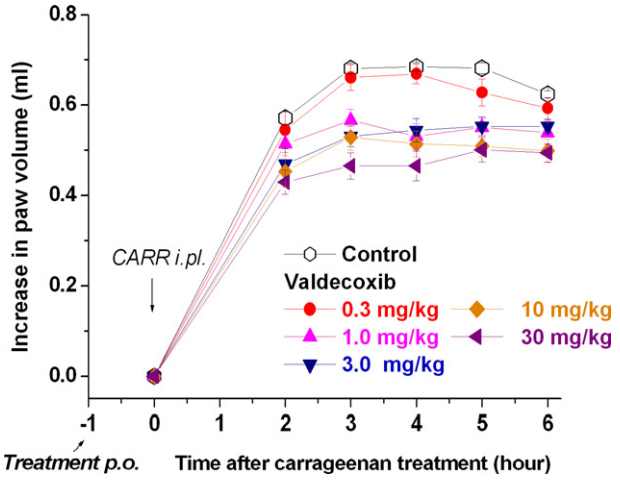

Figure 5. Effect of valdecoxib in paw edema.

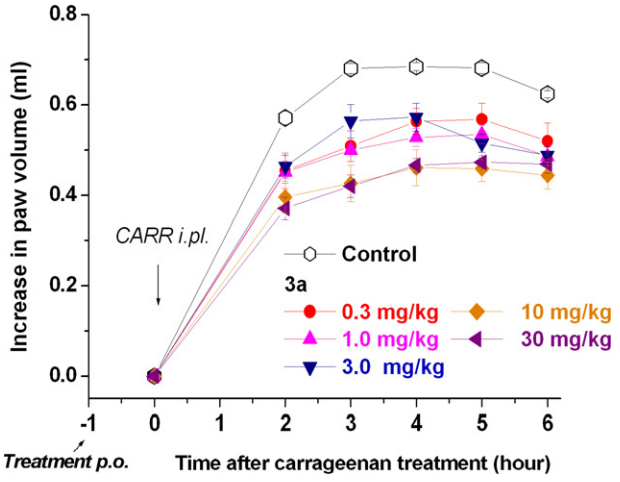

Figure 6. Effect of **3a**·H_2O in paw edema.

strong analgesic effect in the carrageenan-induced mechanical allodynia assay (Figs. 9 and 10).

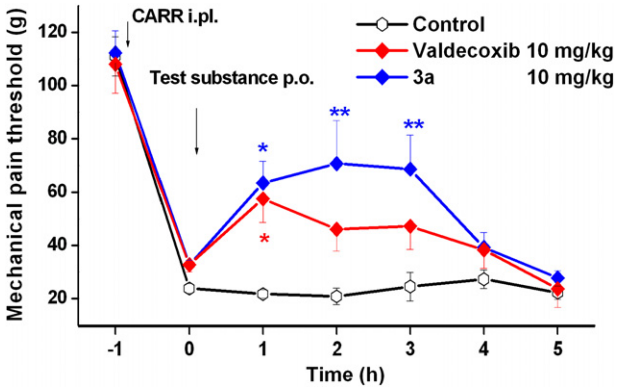

Figure 7. Effects of test compounds in mechanical hyperalgesia.

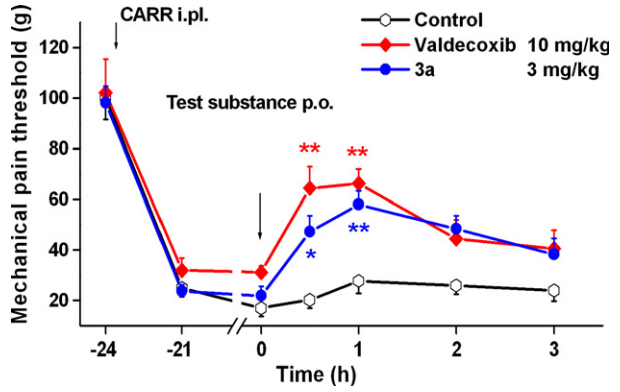

Figure 8. Effects of test compounds in subchronic pain model.

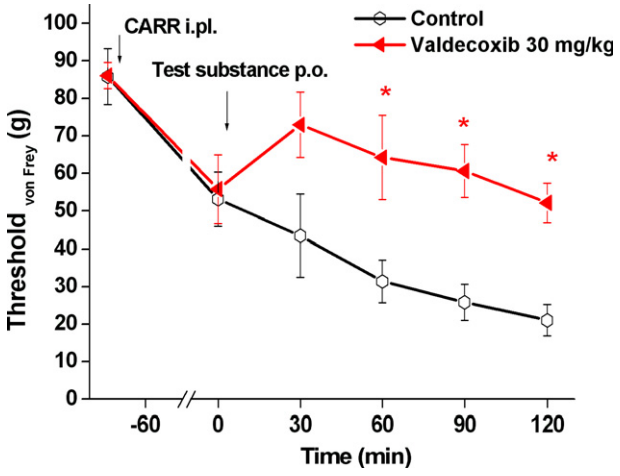

Figure 9. Effect of valdecoxib in mechanical allodynia.

According to the carrageenan–kaolin-induced monoarthritis model both compounds produced almost total inhibition (complete reversal). The analgesic activity had a duration of 2 h (Fig. 11).

In the phenylquinone-induced visceral pain model valdecoxib and **3a**·H_2O are very effective. Test compounds show dose dependent significant analgesic activity: ED_{50}(valdecoxib): 15.5 mg/kg; ED_{50}(**3a**·H_2O): 3.8 mg/kg po (Figs. 12 and 13).

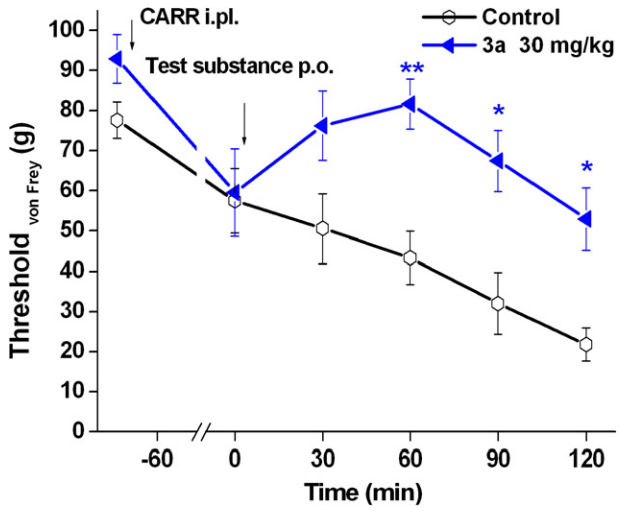

Figure 10. Effect of **3a**·H_2O in mechanical allodynia.

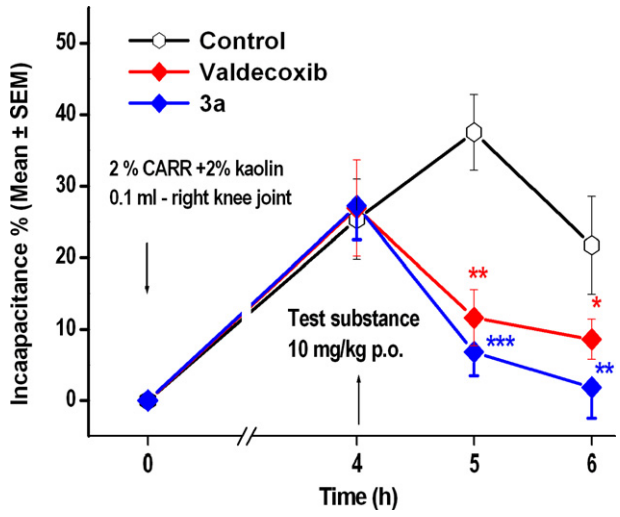

Figure 11. Effect of test compounds in monoarthritis model.

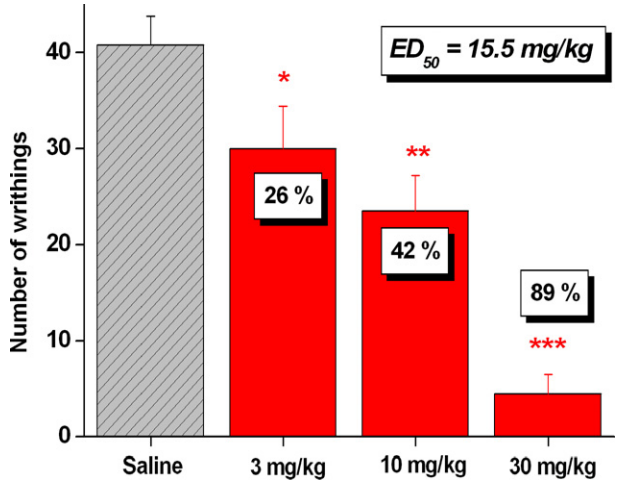

Figure 12. Effect of valdecoxib in writhing test in mice.

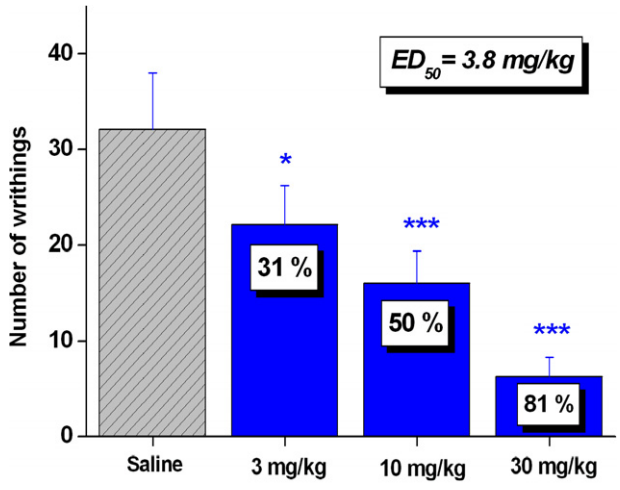

Figure 13. Effect of **3a**·H_2O in writhing test in mice.

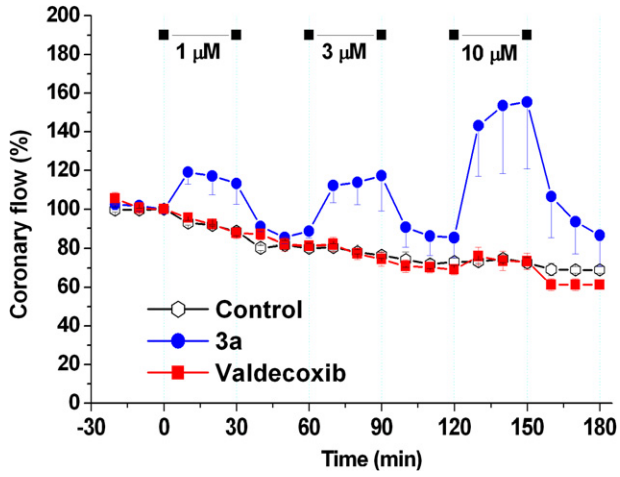

Figure 14. Cardiac effect of valdecoxib and **3a**·H_2O on isolated rabbit heart.

Compound **3a**·H_2O *significantly* increases coronary blood flow dose dependently without altering other parameters (QTS, HR, LPV) in rabbits. Valdecoxib has no effect on coronary blood flow (Fig. 14). The nitric oxide (NO) donor properties of **3a**·H_2O could explain this phenomenon.[18] Neither valdecoxib nor its analogue **3a**·H_2O modified the resting blood pressure of the conscious animals as compared with the solvent-treated group and the values were 84.5 ± 3.54, 82.4 ± 7.96, and 86.45 ± 6.38 mmHg, respectively.

4. Conclusions

Direct analogues of valdecoxib have been prepared to obtain a drug analogue with better properties. *N*-Hydroxy-valdecoxib (**3a**) proved to be an active compound. It is a known metabolite of valdecoxib in human and in mice. The synthesis and the stabilization of **3a** are described. The unsolvated *N*-hydroxy-valdecoxib **3** proved to be unstable. It could be stabilized by recrystallization of compound **3** from a water–ethanol mixture and eliminating the traces of metal ions and free radicals with the help of EDTA and L-ascorbic acid to afford a stable monohydrate **3a**·H_2O. This monohydrate had a weak in vitro COX-2 activity as compared to valdecoxib. Based on in vivo analgesic and anti-inflammatory tests **3a**·H_2O is more potent and has a longer duration of action than the reference compound and significantly increases the coronary blood flow in isolated rabbit heart. The nitric oxide (NO) donor properties of **3a**·H_2O could play a role in its mechanism of action.

5. Methods

In vitro and in vivo testing were performed as given in the literature cited.[19–21] Only modifications are described in this article.

5.1. Spectrophotometric assays with human recombinant COX-2 and bovine COX-1

Enzymatic activities of the human recombinant COX-2 and bovine COX-1 were measured using a spectrophotometric assay based on the oxidation of TMPD during the reduction of PGG2 to PGH2. Valdecoxib and **3a**·H_2O inhibited human recombinant COX-2 in a concentration dependent manner. Inhibition data of valdecoxib and **3a**·H_2O are shown in Table 1 and Figures 2 and 3.

5.2. LPS evoked PGE2 production in human whole blood

The production of PGE2 by LPS-challenged human whole blood has been used to evaluate the efficacy of COX-2 inhibitors in vitro. PGE2 production was measured in heparinized whole blood samples, incubated with LPS for 24 h, as a reflection of the inducible COX activity of monocyte COX-2 (Fig. 4).

5.3. Carrageenan-induced paw edema

The edema was induced in male Wistar rats (130–150 g) by intraplantar injection of carrageenan (CARR; 50 μl of 1% solution) into the right hind paw 1 h after the oral administration of a drug (Figs. 5 and 6). The irritant induced a rapid swelling of the right paw being maximal at 3 h and lasting for 6 h. Right hind paw volume was measured with a plethysmometer (Ugo Basile, type 7150) before and 1, 2, 3, 4, 5, and 6 h after the CARR injection. The increase of paw volume is calculated as a percentage compared with the volume measured immediately before injection of the irritant for each animal. Effectively treated animals show much less edema. The difference of average values between treated animals and vehicle control groups is calculated for each time interval and statistically evaluated.[22]

5.4. Carrageenan-induced mechanical hyperalgesia

CARR-induced hyperalgesia is one of the most frequently applied model of inflammatory pain. The macromolecule induces local inflammation resulting in

persisting hyperalgesia and allodynia. This assay monitors the capacity of the test drugs to reverse hyperalgesia (i.e., decreased threshold to painful stimuli) produced by carrageenan (CARR)-induced inflammation. Male albino rats (Wistar strain—TOXI-COOP Ltd, Hungary–weighing 140–190 g) were used ($n = 6$/group). The mechanical pain threshold of the inflamed hind paw was measured according to the Randall-Selitto method with an 'analgesimeter' (Ugo Basile). The hind paw was compressed with a progressively increasing pressure. The nociceptive threshold is defined as the force, in grams when the animal first vocalized or made a vigorous attempt to remove the paw. Data are presented as the absolute threshold values (means ± SEM) in grams. The percentage reversal of mechanical hyperalgesia was calculated from mean threshold values of a given treatment group as follows:

$$\%\ \text{reversal} = \frac{T_{\text{xh}} - T_{0\text{h}}}{T_{\text{lh}} - T_{0\text{h}}} \times 100,$$

wherein T_{xh} and $T_{0\text{h}}$ are the post- and pre-dose threshold and T_{lh} is the baseline threshold.

- *Acute experiments:* On the day of the experiment the baseline threshold was determined first. After baseline measurements the animals received CARR (100 μl of 2% solution) into the plantar surface of right hind paw. The injected hind paw became maximally inflamed by 2.5–3 h after injection, characterized by edema and decreased mechanical pain threshold. Test compounds were administered orally immediately after 1 h reading. Changes in the threshold were checked at 1, 2, and 3 h following drug administration (Fig. 7).
- *Subchronic experiments:* After baseline measurements the animals received CARR (150 μl mL of 2% solution) ip of right hind paw. The effects of analgesic drugs were studied 24 h after induction of inflammation (in subchronic phase). Test compound was administered orally immediately after 24 h reading (Fig. 8).

5.5. Carrageenan-induced mechanical allodynia in rats

The Electronic von Frey Anesthesiometer was used for the determination of pain sensitivity. The test is performed by applying pressure to the paw through the hand-held force transducer with a sensitive cotton coated rigid tip of the probe. After baseline measurements the animals received CARR (100 μl of 2% solution) into the plantar surface of right hind paw (Figs. 9 and 10).

5.6. Carrageenan–Kaolin-induced monoarthritis in rats

An Incapacitance Tester (ICT) was used to measure the change in weight load on the hind paws before and after induction of monoarthritis, as a measure of functional disability caused by arthritic inflammation and pain. Male WISTAR rats (TOXI-COOP Ltd, Hungary—weighing 120–190 g) were injected with mixture of 2% carrageenan and 2% kaolin (CarrKao) into the joint cavity of the right knee (in 0.1 mL sterile saline) under ether anesthesia ($n = 8$–10/group). Control rats were injected with vehicle.

In therapeutic type experiment drugs were given 4 h after CarrKao injection. Time of measurements: pre-injection of CarrKao, immediately before drug treatment, and 1 and 2 h after the treatment. Change in weight load in the injected and contra-lateral hind limb was measured by ICT device in grams.

The incapacitance was calculated as follows:

$$\%\ \text{incapacitance} = \frac{m_{\text{ll}} - m_{\text{rl}}}{m_{\text{ll}} + m_{\text{rl}}} \times 100,$$

wherein m_{ll} and m_{rl} are the left and right limb weight load (g).

The efficacy of treatment was characterized by percentage reversal of IC% for various time points. Intraarticular administration of CarrKao induced a significant reduction of weight load on the affected leg, with maximum effect at 3–5 h after the injection (Fig. 11).[22]

5.7. Visceral pain model in mice

The phenylquinone (PQ) abdominal contraction assay was used to study the effects of increasing doses of test compounds in a chemo-nociceptive assay.

COX-2 Expression can be induced by lipopolysaccharide (LPS) pre-treatment with 24 h before the study. Inducible COX-2 can be upregulated in acute inflammatory processes. Male NMRI mice (23–30 g, TOXI-COOP Ltd, Hungary) were orally administered with test compound or vehicle 30 min before the challenge with the intraperitoneal injection of 0.02% PQ. Immediately after ip administration of the irritant the animals were placed individually in boxes ($12 \times 12 \times 12$ cm) and the number of abdominal contractions (writhing) were counted for 5–20 min post-injection. Each dose groups consisted of eight animals. The number of these abdominal writhings (constriction of abdomen, turning of trunk, and extension of hind legs) was counted during a 20 min session, beginning 5 min after the injection of PQ. The analgesic activity of the drugs at each dose was determined as a percentage inhibition compared to the degree of writhing in the vehicle controls. The anti-nociceptive response was analyzed by analysis of variance (ANOVA) followed by Tukey's t-test to assess the significance (Figs. 12 and 13).

5.8. Cardiac effect on isolated rabbit heart

New Zealand white rabbits hearts were perfused via the aorta with oxygenated, thermostated Krebs solution. The test compounds were dissolved in the perfusion solution to obtain the requested concentrations. The basic value of coronary blood flow was determined. Afterwards measured amounts of compounds were added to the perfusion liquid and the perfusion was recorded for 30 min at every 10 min. After 30 min perfusion performed without compound the measurement was

repeated with the medium and high amount of compounds (Fig. 14).

5.9. Synthetic procedure for compound 3a

^{1}H NMR spectra were obtained on a Varian Unity Inova 300 spectrometer. Chemical shifts are reported in parts per million relative to TMS as internal standard. MS spectra were measured on Finnigan Mat 95 SQ and 95 XP devices.

5.9.1. 4-(5-Methyl-3-phenylisoxazol-4-yl)benzenesulfonyl chloride (2a). Compound **1** (8.00 g, 34.0 mmol) was added to chlorosulfonic acid (22.6 mL, 340 mmol) at 5 °C in small portions over 30 min and the mixture was left to stand for 5 h at room temperature. The conversion was followed by TLC: toluene/EtOAc 12:1. After the completion of the reaction, the mixture was poured into crushed ice and the resulting aqueous suspension was extracted with CH_2Cl_2 (2×90 mL). The combined organic layers were washed with brine, dried over anhydrous $MgSO_4$, filtered, and concentrated in vacuo to give a crude product. Recrystallization from cyclohexane to remove *meta*-isomer (**2b**) provided the pure *ortho*-sulfonyl chloride **2a** (7.26 g, 64%). TLC: toluene/EtOAc 12:1, silica, $R_f = 0.55$. MS (EI) $M^+ = 333$, ^{1}H NMR (300 MHz, DMSO-d_6, 30 °C) δ 7.71–7.64 (m, 2H); 7.49–7.34 (m, 5H); 7.24–7.17 (m, 2H); 2.45 (s, 3H) ppm.

5.9.2. *N*-Hydroxy-4-(5-methyl-3-phenylisoxazol-4-yl)benzenesulfonamide monohydrate (3a·H$_2$O). A suspension of hydroxylamine hydrochloride (6.88 g, 99.0 mmol) in dioxane (50 mL) was added to a solution of sodium acetate (8.12 g, 99.0 mmol) in water (25 mL). To this mixture, compound **2a** (11.0 g, 33.0 mmol) in dioxane (50 mL) was added at 10 °C dropwise, over a period of 30 min and it was then stirred for additional 30 min at room temperature. The reaction mixture was diluted with water (500 mL) and shaken for 2 h. The suspension was filtered off, the filtrate was dissolved in EtOAc (200 mL), extracted with an aqueous solution (40 mL) of 5 m/m% Na_2EDTA, with water (40 mL) and finally with brine (20 mL) and evaporated in vacuo. The residue was dissolved in EtOH (90 mL), decolorized by activated carbon (1 g), filtered, and water (270 mL) containing ascorbic acid (3 g) was added to the solution at 60 °C. The mixture was cooled to 5 °C, the precipitate formed was collected by filtration, washed with water and dried to provide the title compound **3a**·H$_2$O (7.80 g, 68%). Mp 95–110 °C. MS (EI) $M^+ = 330$, ^{1}H NMR (300 MHz, DMSO-d_6, 30 °C) δ 9.66 (s, 2H); 7.87–7.80 (m, 2H); 7.50–7.32 (m, 7H); 2.49 (s, 3H) ppm.

5.10. Crystal structure determination of 3a·H$_2$O

Crystallographic data (excluding structure factors) for the structure in this paper have been deposited with the Cambridge Crystallographic Data Centre as supplementary publication No. CCDC 660035.

Data reduction was obtained from Harms, K. (1996) XCAD4 Data Reduction Programme for CAD4 Diffractometers, Philipps-Universität Marburg, Germany. The structure was elucidated by SHELXS: Sheldrick, G. M. SHELXS-97, Program for Crystal Structure Solution, University of Göttingen, Germany, 1997. Structure refinement was carried out by Sheldrick, G. M. SHELXL-97, Program for Crystal Structure Refinement, University of Göttingen, Germany, 1997.

A plate-like single crystal of **3a**·H$_2$O was selected for X-ray crystal structure determination. A crystal of FT_WA was mounted on a glass fiber. Cell parameters were determined by least-squares of the setting angles of 25 ($20.24 \leqslant \theta \leqslant 24.36°$) reflections. Crystal data: $C_{16}H_{16}N_2O_5S$, F_{wt}: 348.37, colorless, plate, size: $0.22 \times 0.11 \times 0.09$ mm, monoclinic, space group $P2_1/c$, $a = 7.659(1)$ Å, $b = 23.510(1)$ Å, $c = 9.148(1)$ Å, $\alpha = 90°$, $\beta = 95.65(1)°$, $\gamma = 90°$, $V = 1639.2(3)$ Å^3, $T = 295(2)$ K, $Z = 4$, $F(000) = 728$, $D_x = 1.412$ mg/m^3, $\mu = 2.022$ mm^{-1}. Intensity data were collected on a Enraf-Nonius CAD4 diffractometer (graphite monochromator; Cu-Kα radiation, $\lambda = 1.54184$ Å) at 295(2) K in the range $3.76 \leqslant \theta \leqslant 75.58°$ using $\omega/2\theta$ scans. The intensities of three standard reflections were monitored regularly (every 60 min). The intensities of the standard reflections remained constant within experimental error throughout the data collection. A total of 3655 reflections were collected of which 3344 were unique [$R(\text{int}) = 0.0077$, $R(\sigma) = 0.0528$]; intensities of 2021 reflections were greater than $2\sigma(I)$, completeness to $\theta = 0.981$. No absorption correction was applied to the data. The structure was solved by direct methods (and subsequent difference syntheses). Anisotropic full-matrix least-squares refinement on F^2 for all non-hydrogen atoms yielded $R_1 = 0.0406$ for 2029 [$I > 2\sigma(I)$] and $R_1 = 0.0855$ and $wR_2 = 0.1089$ for all (3352) intensity data. The maximum and minimum residual electron density in the final difference map were 0.25 and -0.26 e Å^{-3}. The weighting scheme applied was $w = 1/[\sigma^2(F_o^2) + (0.055P)^2 + 0.0000P]$ where $P = (F_o^2 + 2F_c^2)/3$. Hydrogen atomic positions were calculated from assumed geometries except –OH and –NH H atoms that were located in difference maps. Hydrogen atoms were included in structure factor calculations but they were not refined. The isotropic displacement parameters of the hydrogen atoms were approximated from the U(eq) value of the atom they were bonded to.[23]

Acknowledgments

We thank Drs. Gábor Tárkányi and Tamás Gáti for the measurements and elucidations of the NMR spectra. We also thank Sándor Lévai for his contribution to the stability assays and HPLC measurements.

References and notes

1. Vane, J. R. *Nature (New Biol.)* **1971**, *231*, 232.
2. Raz, A.; Wyche, A.; Siegel, N.; Needleman, P. *J. Biol. Chem.* **1988**, *263*, 3022.
3. Fu, J. R.; Masferrer, J. L.; Seibert, K.; Raz, A.; Needleman, P. *J. Biol. Chem.* **1990**, *265*, 16737.

4. Battistini, B.; Botting, B.; Bakhle, Y. S.. *Drug News Perspect.* **1994**, *7*, 501.
5. Xie, W.; Chipman, J. G.; Robertson, D. L.; Erikson, R. L.; Simmons, D. L. *Proc. Natl. Acad. Sci. U.S.A.* **1991**, *88*, 2692.
6. Kujubu, D. A.; Fletcher, B. S.; Varnum, B. C.; Lim, R. W.; Herschman, H. R. *J. Biol. Chem.* **1991**, *266*, 12866.
7. O'Banion, M. K.; Sadowski, H. B.; Winn, V.; Young, D. A. A. J.. *Biol. Chem.* **1991**, *266*, 23261.
8. Vane, J. R.; Botting, R. M. . *Adv. Prostaglandin, Thromboxane, Leukot. Res.* **1995**, *23*, 41.
9. Allison, M. C.; Howatson, A. G.; Torrance, C. J.; Lee, F. D.; Russell, R. I. G. *N. Engl. J. Med.* **1984**, *310*, 563.
10. Penning, T. D.; Talley, J. J.; Bertenshaw, S. R.; Carter, J. S.; Collins, P. W.; Docter, S.; Graneto, M. J.; Lee, L. F.; Malecha, J. W.; Miyashiro, J. M.; Rogers, R. S.; Rogier, D. J.; Yu, S. S.; Anderson, G. D.; Burton, E. G.; Cogburn, J. N.; Gregory, S. A.; Koboldt, C. M.; Perkins, W. E.; Seibert, K.; Veenhuizen, A. W.; Zhang, Y. Y.; Isakson, P. C. *J. Med. Chem.* **1997**, *40*, 1347.
11. *Analogue-Based Drug Discovery*; Fischer, J., Ganellin, C. R., Eds.; Wiley-VHC Verlag GmbH & Co. KGaA, 2006.
12. Talley, J. J.; Brown, D. L.; Carter, J. S.; Graneto, M. J.; Koboldt, C. M.; Masferrer, J. L.; Perkins, W. E.; Rogers, R. S.; Shaffer, A. F.; Zhang, Y. Y.; Zweifel, B. S.; Seibert, K. *J. Med. Chem.* **2000**, *43*, 775.
13. Uddin, Md. J.; Rao, P. N. P.; Knaus, E. E. *Bioorg. Med. Chem.* **2003**, *11*, 5273.
14. Zarghi, A.; Rao, P. N. P.; Knaus, E. E. *Bioorg. Med. Chem.* **2007**, *15*, 1056.
15. Zhang, J. Y.; Yuan, J. J.; Wang, Y. F.; Bible, R. H.; Breau, A. P. *Drug Metab. Dispos.* **2003**, *31*, 491.
16. Yuan, J. J.; Yang, D. C.; Zhang, J. Y.; Bible, R.; Karim, A.; Findlay, J. W. A. *Drug Metab. Dispos.* **2002**, *30*, 1013.
17. Bonner, F. T.; Ko, Y. *Inorg. Chem.* **1992**, *31*, 2514.
18. Zamora, R.; Grzesiok, A.; Weber, H.; Feelisch, M. *Biochem. J.* **1995**, *312*, 333.
19. Gierse, K.; Hauser, S. D.; Creely, D. P.; Koboldt, C. M.; Rangwala, S. H.; Isakson, P. C.; Siebert, K. *Biochem. J.* **1995**, *305*, 479.
20. *Drug Discovery and Evaluation Pharmacological Assays*; Vogel, H. G., Vogel, W. H., Eds.; Springer-Verlag: Berlin, Heidelberg, 1997.
21. Atkinson, D. C. *Arch. Int. Pharmacodyn. Ther.* **1971**, *193*, 391.
22. Statistics: Data were analyzed by two-way ANOVA followed by Tukey's (HSD) post hoc test, comparing drug-treated with vehicle-treated animals. Significance was considered at $p < 0.05$ level ($^{*}p < 0.05$; $^{**}p < 0.01$; $^{***}p < 0.001$).
23. Neutral atomic scattering factors and anomalous scattering factors are taken from: *International Tables for X-ray Crystallography*; Wilson, A. J. C., Ed.; Kluwer Academic Publishers: Dordrecht, 1992; Vol. C,, Tables 6.1.1.4, pp 500–502, 4.2.6.8, pp 219–222 and 4.2.4.2, pp 193–199.